Influence of the Thermophysical Model on the CFD Analysis of Oil-Cooled Transformer Windings

Elisabetta Salerno, Adriano Leonforte, Diego Angeli*

DISMI - Dipartimento di Scienze e Metodi dell'Ingegneria, Università di Modena e Reggio Emilia - Via Amendola 2, Pad. Morselli, 42122 Reggio Emilia (Italy)

*corresponding author, e-mail: diego.angeli@unimore.it

Abstract. A disc-type winding of an oil-immersed power transformer is modeled with Computational Fluid Dynamics. Different approaches are implemented to evaluate the feasibility of the Boussinesq approximation: (i) constant fluid properties, (ii) variable viscosity and thermal diffusivity and (iii) temperature-dependent fluid properties. Temperature and flow distributions are reconstructed and put into relation with physical phenomena and model assumptions. Their comparison suggests that numerical results are fairly sensitive to the thermophysical model as long as the buoyancy force is a relevant component of the flow. Nonetheless, all the cases converge to very close predictions of the hot-spot value and location, with possibly positive implications for the use of reference parameters when deriving flow and heat transfer correlations for this topic.

Key Words: Power transformers, oil properties, buoyancy-driven flows, CFD, Boussinesq approximation

1. Introduction

Temperature and coolant flow distribution are fundamental aspects in the design and operation of oil-immersed power transformers. Losses inherent to the electro-magnetic circuit cause heat production in the core, windings and structural parts; when excessive temperatures are reached, the insulation material rapidly gets aged and, ultimately, results in transformer failure. Therefore, the cooling system represents a key component of the transformer assembly, its specific configuration to be founded on accurate evaluation of thermal and hydraulic issues entangled with the electric scheme. In particular, estimating the value and location of the maximum temperature occurring in winding paper insulation, the so-called hot-spot, is of primary importance since it dictates transformers reliability and life expectancy [1].

International Standards [1, 2] give practical indications for the calculation of the hot-spot temperature during steady state or transient operation. However, those methods often prove to be quite unreliable [3, 4], since they are based on average temperatures of the windings and of the oil measured in a few specific points of the cooling circuit. Even direct measurements of the hot-spot can suffer of large errors as its exact position is not known a priori. Hence, strategies are required that are more precise for a correct management and prediction of transformers thermal behaviour.

Due to the complexity of carrying out experiments on transformers, research tools applied to this topic are mainly numerical. Thermal modeling techniques used in this field include reduced order modeling, thermal networks (THNM) and Computational Fluid Dynamics (CFD). Between the two

approaches, CFD is the most suited to investigate the physical phenomena affecting the cooling performance of transformers, since it provides detailed information for their interpretation. The attention of CFD studies has been focused in particular on disc-type windings, where the oil flows in both horizontal and vertical channels separating the heating surfaces. For example, it was shown that in such a configuration, the oil temperature is not always well mixed in the cooling ducts; on the contrary, hot-streaks depart from disc surfaces and considerably influence the heat transfer downstream, and large recirculation zones appear at the entrance of horizontal channels when increasing the oil flow rate [5–8]. On the other hand, the large computational costs associated with CFD discourage its use for extensive parametric studies on transformer windings, or for full scale analysis of the entire transformer cooling circuit. Nevertheless, useful correlations can be derived from CFD analysis on separate transformer elements; those can be implemented to improve the accuracy of reduced order and thermal network models, which offer less computational requirements for large scale analyses. For this purpose, data reduction and generalization need well-defined dependent and independent parameters. The use of constant against temperature-dependent thermophysical properties for the oil is an important issue in this sense, but even though the Boussinesq approximation is often applied in CFD studies of disc-type windings, its implications are poorly debated.

To this aim, a CFD analysis is brought forward here to assess the effect of the choice of the thermophysical model on the numerical predictions of flow and heat transfer in a disc-type winding. The reference case is taken from a previous study in the literature [7], for which experimental and numerical data are available. The validity of the Boussinesq approximation is discussed, and the effect of setting constant or temperature-dependent viscosity and thermal diffusivity in the CFD model is assessed through cross-comparison and benchmarking with the aforementioned data. Finally, an attempt is made at providing reasonable guidelines for engineering calculations. Such indications could also be beneficial for future parametric analyses, aimed at extracting reliable integral correlations for friction losses and convective heat transfer, which are of fundamental importance for the success of reduced-order models of the cooling circuit of power transformers.

2. Case study

A geometric section of the disc-type winding investigated [7] is illustrated in Figure 1. The winding is composed of 4 passes, each containing 19 discs and 20 horizontal ducts. Vertical channels of different radial width are interposed between the discs and the surrounding cylinders (these ones not represented). Cardboard washers of 1 mm height are inserted to separate passes at alternating inner and outer location, i.e. blocking the oil passage in the inner and outer vertical duct, in order to induce zig-zag cooling. Washers are arranged so that the oil enters pass 1 and leaves the winding through the outer vertical channel. An entry region with 2 extra discs and 3 horizontal ducts is present below the first pass, which is functional for the development of realistic temperature and velocity profiles of the oil flow. Inlets to the entry region are located at both the inner and outer vertical channels. The internal structure of the discs is represented, made of 18 copper conductors that are individually wrapped with paper insulation. The reader is referred to [7] for further winding details.

3. Numerical model

3.1. Governing equations and discretization schemes

The conservation equations of mass, momentum and energy can be written as follows:

$$\frac{\partial \rho}{\partial t} + \nabla(\rho \mathbf{u}) = 0 \tag{1}$$

$$\rho \frac{\partial \mathbf{u}}{\partial t} + \rho \mathbf{u} \cdot \nabla \mathbf{u} = -\nabla p + \mu \nabla^2 \mathbf{u} + \mathbf{g} (\rho - \rho_{\mathrm{ref}}) \tag{2}$$

$$\frac{\partial(\rho c_p T)}{\partial t} + \nabla(\rho c_p \mathbf{u} T) = \nabla(k \nabla T) \tag{3}$$

Under the Boussinesq approximation, the dependence of ρ on T can be linearized as follows:

$$\rho - \rho_{ref} = -\beta (T - T_{ref}) \tag{4}$$

The Boussinesq approximation has been implemented in both its canonical formulation and in a modified version, where temperature-dependence of thermal and momentum diffusivity are taken into account. Furthermore, a third case without adopting the Boussinesq approximation, i.e. all the fluid properties considered variable, has been performed for comparison with the aforementioned cases (see Section 3.2). To take into account the temperature distribution inside the discs of the winding, the heat conduction equation in a solid is solved:

$$\frac{\partial(\rho c_p T)}{\partial t} = -\nabla(k \nabla T) + S_E \tag{5}$$

The source term S_E, which represents the energy losses in the windings, is imposed in the copper conductors of the discs.

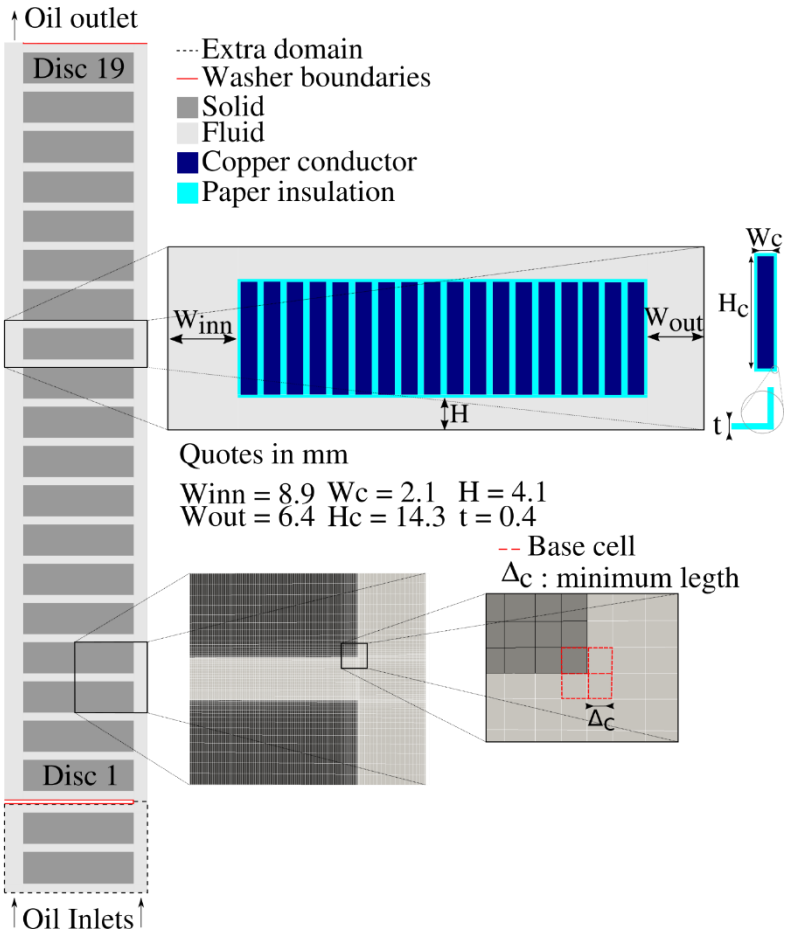

Figure 1. Schematic view of the investigated case. Fluid and solid domains of the first pass and entry-region are depicted, together with the main dimensions and details of the mesh topology.

The above equations have been numerically solved under steady-state and laminar flow conditions via the open source OpenFOAM computational toolbox [9], which is based on the finite-volume method. A conjugate heat transfer solver which employs the Semi-Implicit Method for Pressure Linked Equations (SIMPLE) algorithm is adopted together with second-order schemes for discretization.

3.2. Thermophysical models

As already mentioned, flow and heat transfer in the winding are evaluated with three different approaches for the fluid properties: (i) the Boussinesq approximation in its canonical formulation, (ii) variable viscosity and thermal diffusivity only (here labeled as "modified Boussinesq"), and (iii) temperature-dependent properties. For the first two cases, the average bulk temperature of the oil, computed from energy balance, is used as the reference temperature for the evaluation of the constant properties. Depending on the approach, two different implementations of the conjugate heat transfer of OpenFOAM are alternatively used, belonging to the original and the extended version (the *foam-extend* project, which is a fork of the original version), respectively, with consequent different specification of the fluid input parameters, as summarized in Table 1. Oil and solid properties are taken and derived from [7].

Table 1. Thermophysical models for the three cases investigated.

	Boussinesq	modified Boussinesq	Variable properties
OpenFOAM version	extended	extended	original
Fluid input parameters:			
Reference temperature, T_{ref} [°C]	63.52	63.52	-
Thermal expansion coefficient, β [K^{-1}]	8.29e-4	8.29e-4	-
Viscosity, dynamic or kinematic, μ [Pa s] or ν [$m^2 s^{-1}$]	7.77e-6 (ν)	temperature-dependent[a] (ν)	temperature-dependent[a] (μ)
Density, ρ [kg m^{-3}]	859.01	859.01	temperature-dependent[b]
Thermal conductivity, k [W m^{-1} K^{-1}]	(auto. computed)	(auto. computed)	temperature-dependent[b]
Specific heat, c_p [J kg^{-1} K^{-1}]	2012.43	2012.43	temperature-dependent[b]
Prandtl number, Pr	106	temperature-dependent[a]	(auto. computed)

[a] 2nd order polynomial fit from expressions in [7].

[b] Correspondent original expression in [7].

It should be pointed out that the Boussinesq approximation cannot be considered valid in the present problem from a theoretical standpoint. In fact, temperature differences are estimated to be at least two times higher than those prescribed by criteria in [10] for the introduction of acceptable errors in the equations. However, the feasibility of such approximation is studied anyway for its practical implications.

3.3. Meshing and BCs

In order to reduce the computational requirements, the problem is supposed to be axisymmetric. Therefore, only a thin slice of the winding with 4° angular extension has been reproduced and solved. A conformal structured grid with non-uniform cell grading is used for meshing the domain, with just one cell in the azimuthal direction. The smallest cells (base cells) are located at the sharp edges of the discs as reported in Figure 1. Special attention has been paid in controlling the mesh grading in horizontal ducts, due to the possible onset of Rayleigh–Bénard-like flow structures.

A fixed inlet oil temperature of 46.7 °C is imposed for all the cases investigated in this work, as in [7]. At the two inlets of the entry-region a total mass flow rate of 0.78 kg/s is enforced by specifying the inlet bulk velocity. The mass flow rate value, which is referred to a 360° cylindrical domain, is kept fixed for all the cases considered, therefore slightly different inlet velocities are set from case to case to take into account the appropriate density value. An average pressure condition, $p_{avg} = 0$, is imposed at the winding outlet. The no-slip condition is specified on all the fluid-solid boundaries, with all other solid walls set as adiabatic. A uniform heat source is specified in the copper conductor region, in order to reproduce the value of 676.9 W/disc reported in [7], which is valid for a 360° domain. In the azimuthal direction, axial symmetry is imposed.

To check the validity of the numerical models, a grid convergence study has been performed on the first pass, entry region included, in terms of percentage deviation of the overall pressure drop and Nusselt number. Three grids with different resolution have been tested, by rescaling the mesh with respect to the base cell, while keeping the same mesh grading. A refinement factor of 2 has been considered for the length of the base cell, thus implying a successive increase of the total cell count by a factor 4. The standard Boussinesq approximation has been retained for this subtask. Information on the meshes and results of the grid convergence study are reported in Table 2, where percentage deviations are indicated towards the Refined Mesh. Since for the Intermediate Mesh deviations are obtained which are below 1% for both parameters - one half than those exhibited by the Coarsest Mesh - the Intermediate Mesh has been chosen as reference in the evaluation of the complete winding, for which the overall grid consists of 5583050 cells.

Table 2. Details and results of the grid independence study on the first pass.

	Coarse Mesh	Intermediate Mesh	Refined Mesh
Δ_c [mm]	0.08	0.04	0.02
Cell number	370867	1521930	6087720
p_{avg} on inlet (% deviation)	-2.21 %	-0.9 %	-
Nusselt (% deviation)	-0.43 %	-0.2 %	-

4. Results and discussion

A comparison between the distributions of the average disc temperature for the explored cases is plotted in Figure 2, together with the data reported in Torriano et al. [7] for the correspondent axisymmetric model. A general rapid increase in the disc temperature can be observed along the first pass, with a pronounced local maximum near the top. Beyond the washer the temperature drops, and subsequently increases again with a milder slope. Hence, a smaller local maximum is obtained in the second pass, still residing near the top discs. The present data denote appreciable differences in this part of the winding with respect to the results of Torriano et al. [7]: as reported in Table 3, the location of the hottest disc in the first pass is only slightly shifted (disc 18 for all present cases against disc 17 in [7]), while its corresponding average temperature spans a range of 11 °C depending on the model assumptions: the highest value is exhibited by the canonical Boussinesq prediction, with a 21% percentage deviation from the results of Torriano et al., which exhibit the lowest value. Following a partial re-alignment, the temperature curves deviate again in the upper portion of the second pass: with the canonical Boussinesq model, a local maximum of moderate entity is detected at disc 35, the discs further downstream being considerably colder; in the other cases, higher temperatures are obtained at taller heights, without a significant decrease of temperature below the pass outlet.

Those discrepancies are completely levelled out in the third pass, where we observe almost coincident temperature distributions immediately above the washer. Their trend roughly replicates the one in the previous pass, but appears as stretched towards hotter values and with a steeper increase. As confirmed by Table 3, the global hot-spot of the winding lies in this pass for all the cases considered, at about the same location (discs 51-52, i.e. at ¾ of the pass height) and with very close values (percentage deviations < 4%). Comparably high temperatures are obtained also in the fourth pass at two locations: in the lowermost disc and, again, at three-quarter height of the pass. In fact, the disc temperature distributions denote a pronounced z-shape in the last pass, with some differences in the temperature excursion from case to case. The modified Boussinesq and variable properties cases show very similar behaviours for the whole second half of the winding: mutual deviations in the average temperature of the discs are obtained which are largely below 1.5%. Their differences with the data in [7] are limited to 3% in this region, while with the canonical Boussinesq approximation slightly larger discrepancies (up to 5%) are observed.

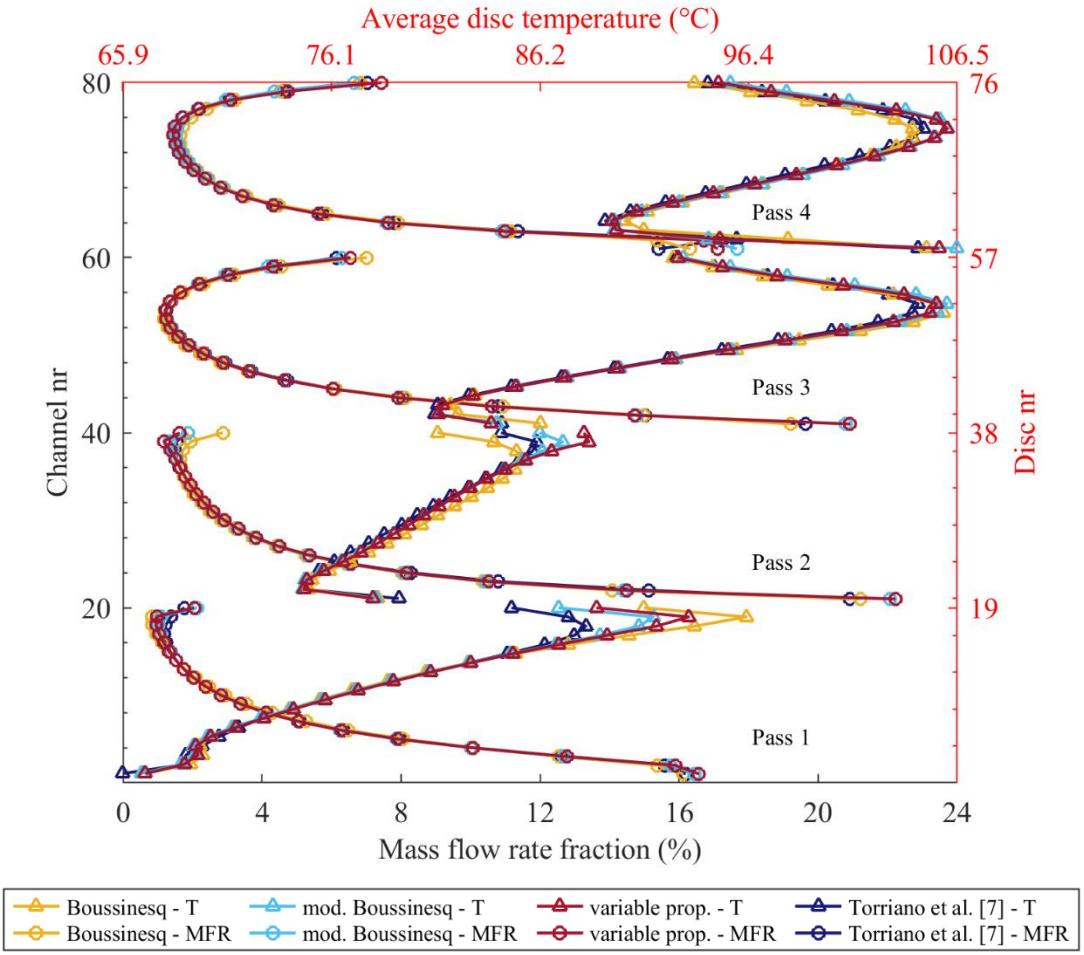

Figure 2. Average disc temperature (T) and mass flow rate (MFR) distributions. Entry region not included.

Temperature distributions can be partially understood by considering the mass flow rate (MFR) distributions collated in Figure 2, which were calculated from average velocities at the duct centres according to [7]. The first two passes of the winding have a strongly asymmetric oil repartition among the horizontal ducts, revealing a strong contribution of the buoyancy force in driving the pressure drop between vertical channels [5, 6]. In the upper half of the winding a more even distribution is present; this can be ascribed to the higher temperature of the incoming oil, which scales down the hydrostatic pressure difference at the bottom of the passes. The difference between the cross sections of the inner and outer vertical channels may also have a role in rearranging the flow.

Table 3. Hot-spot values and locations. Percentage deviations (Δ %) are calculated for $T_{hot\text{-}spot} - T_{inlet}$ temperature differences towards those in Torriano et al. [7]. Global hot-spots are highlighted.

	Torriano et al.		Boussinesq			modified Boussinesq			variable properties		
Local hot-spot	T (°C)	disc #	T (°C)	Δ %	disc #	T (°C)	Δ %	disc #	T (°C)	Δ %	disc #
Pass 1	99.4	17	110.2	20.6	18	104.3	9.4	18	106.5	13.4	18
Pass 2	95.0	35	94.3	-1.4	35	97.3	4.7	37	98.9	9.1	37
Pass 3	**115.0**	**52**	**117.6**	**3.8**	**51**	**117.5**	**3.6**	**52**	**116.7**	**2.5**	**52**
Pass 4	113.8	71	113.5	-0.5	70	115.7	2.8	71	115.6	2.7	71

A correspondence between the profiles of mass flow rate fraction and disc temperature can be noticed: poor oil flow through a channel implies a bad cooling of the adjacent discs and, conversely, high flow rates help keeping the disc temperatures low. The first disc of passes 2 and 3 and the first two discs of pass 4 represent an exception: temperature contours in Figure 3, referred to the fluid domain of the standard Boussinesq case and similar for the other ones, evidence the presence of hot-streaks which are conveyed from one vertical channel to the other one through the lowest horizontal ducts of each pass, starting from pass 2. As a consequence, relatively high temperatures are obtained in the first discs of those passes though the MFR in the surrounding channels is high.

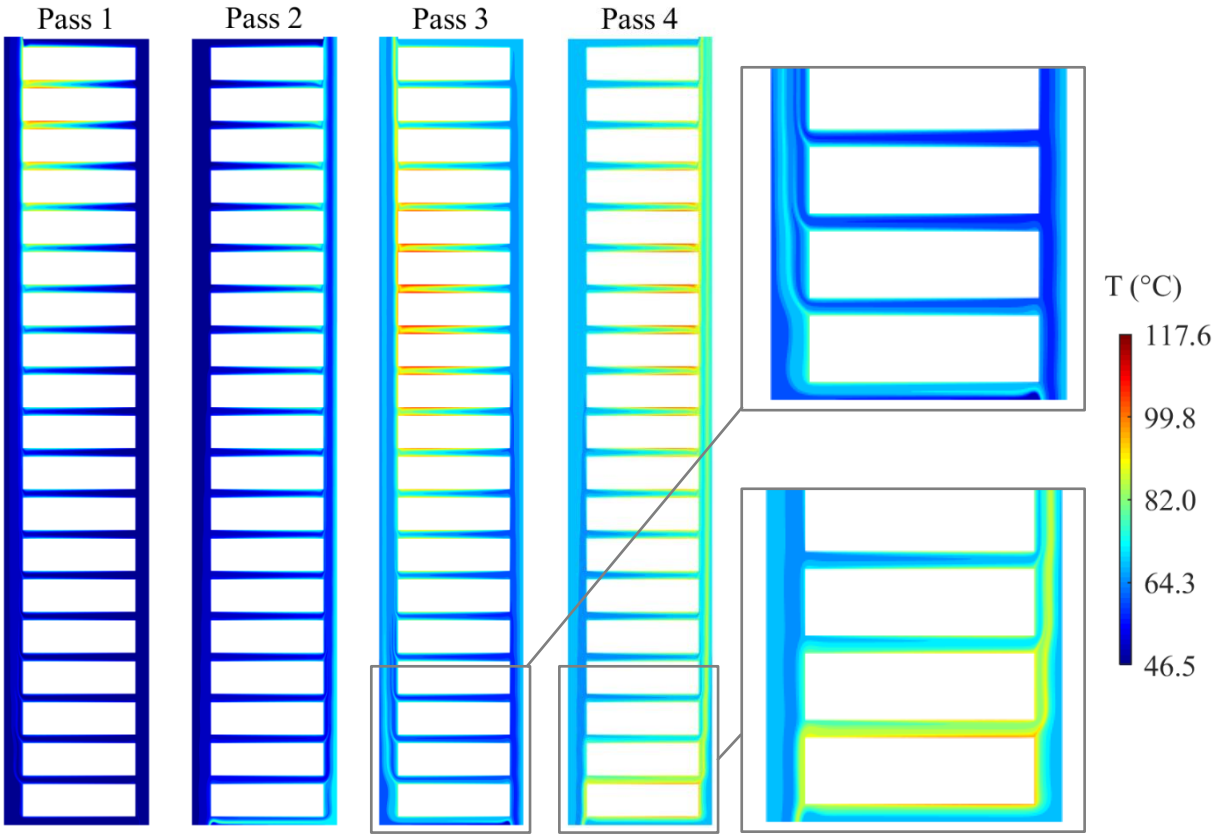

Figure 3. Temperature contours of the fluid domain for the standard Boussinesq case.

Of major relevance are the shifts in MFR values between the inspected cases in regions where the oil flow is scant. Despite an apparent overlap of the curves, in pass 1 percentage deviations from 7 to 22% exist between the present cases for what concerns the minimum MFR fraction. Such deviations reverberate onto the temperature gradient across the channels. In turn, these deviations are at the basis of the significant scatter of temperatures observed in Figure 2 for the first pass. In the same region, even larger deviations are encountered between the mass flow rates reported in [7] and those predicted with variable properties; although these models are based on identical assumptions, simulations in [7] were performed in separate runs (one per pass). It is so inferred that the boundary conditions imposed at each pass outlet could influence the flow behaviour in their proximity, resulting in a modification of the flow and temperature distributions when compared to solutions from the whole geometry. As visible in Figure 2, this is particularly true in the lower passes, i.e. far from the winding outlet.

The Boussinesq approximation, in both the canonical and modified formulation, keeps affecting flow repartition beyond the first pass. However, relevant effects on the temperature field are restricted to pass 2, since discrepancies occur near the top, where oil velocities are small due to buoyancy driven flow. Shifts in MFR curves that emerge in pass 4 in the standard Boussinesq case are less impacting

because the absolute values of the mass flow rate minima are globally higher. The picture met in the third pass is clearly different. Here, temperatures closer to the reference value used for the Boussinesq cases are found on average, so producing (i) a good match between velocity profiles and MFR data, and (ii) more significantly, consistent predictions of the hot-spot value and location.

As an additional check for model validity, experimental data provided in [3] for the same winding are compared to numerical results in Table 4. Average winding temperature rises obtained in the present study are 7% lower than the measured one, a difference possibly ascribable to the axisymmetric assumption, while good agreement is achieved between top oil temperatures.

Table 4. Comparison with experimental data [3] from temperature rise test on the real winding (ambient temperature = 30.2 °C). Percentage deviations (Δ %) are calculated towards those values.

	exp. data [3]	Boussinesq		mod. Boussinesq		variable properties	
	θ (K)	θ (K)	Δ %	θ (K)	Δ %	θ (K)	Δ %
Average winding temperature rise	61.6	57.3	-6.9	57.3	-7.0	57.3	-7.0
Top oil temperature rise	50.2	49.2	-2.0	49.5	-1.4	49.4	-1.7

5. Concluding remarks

The feasibility of the Boussinesq approximation when modeling disc-type windings of oil-cooled transformers has been investigated by means of CFD. A case study from the literature has been taken for reference, and replicated in its axisymmetric simplification with three different assumptions for the temperature dependency of thermophysical properties. In theoretical terms, the Boussinesq approximation cannot be considered valid in its canonical formulation throughout the temperature range of the problem, as dictated by the relations used for the thermophysical properties of the oil. Numerical results have given evidence of such a consideration: relatively to the case with variable properties, a good agreement has been obtained where the oil temperature is close, on average, to the reference one; as opposite, relevant deviations have been encountered for the mass flow rate in other regions. Those differences are particularly relevant when established in channels crossed by scant oil flow, since they amplify the discrepancies between temperatures of the adjacent discs; it is the case of the lowermost passes of the winding, where buoyancy effects determine a mass flow distribution which is strongly asymmetrical. While a generally better match has been found when fluid viscosity and thermal diffusivity are allowed to vary, all the three models produce consistent predictions of the hot-spot value and location. Hence, it is argued that the use of thermophysical properties computed at the average temperature of the oil can be a proper choice as far as the hot-spot determination is the major concern. The modified formulation of the Boussinesq approximation is more adequate instead if correlations should be extracted for friction losses and convective heat transfer. Further investigations are required to check the portability of those considerations to different flow regimes.

References

[1] IEC 60076-7:2018 Power transformers – Part 7.
[2] IEC 60076-2:2011 Power transformers – Part 2.
[3] Picher P, Torriano F, Chaaban M, Gravel S, Rajotte C and Girard B 2010 *CIGRE Conference (Paris, France)*, A2-305.
[4] Laneryd T, Gustafsson A, Kranenborg E J, Duarte P, Calil W, Zacharias J and Mendes J C 2014 *CIGRE WorkSpot VII Conference (Rio de Janeiro, Brazil)*.
[5] Kranenborg E J, Olsson C O, Samuelsson B R, Lundin L Å and Missing R M, 2008 *Proc. 5th European Thermal-Sciences Conf. (The Netherlands)*.
[6] Torriano F, Chaaban M and Picher P 2010 *Appl. Therm. Eng.* **30** 2034–44.
[7] Torriano F, Picher P and Chaaban M 2012 *Appl. Therm. Eng.* **40** 121–31.
[8] Skillen A, Revell A, Iacovides H and Wu W 2012 *Appl. Therm. Eng.* **36** 96–105.
[9] Weller H G, Tabor G, Jasak H and Fureby C 1998 *Comp. Phys.* **12** 620–631.
[10] Gray D D and Giorgini A 1976 *Int. J. Heat Mass Transf.* **19** 545–51.